

4.4 Expansion Fans and Compressions: Formal Theory.

The ideas presented in the previous section can be formalized using the method of characteristics for steady, 2D, shallow flow. This methodology has been used widely in the field of aerodynamics to describe supersonic flow (Courant and Friedrichs 1948). A simple reinterpretation of variables in the governing equations leads to solutions of the shallow water equations, with or without rotation. The irrotational case is particularly simple and leads to descriptions of the marine layer expansion fans and compressions that are elegant and that capture most of the important physical mechanisms. The methodology can be extended to account for rotation but the governing equations for this case (Appendix C) are less transparent.

(a) Summary of the Method of Characteristics

The essential ideas underlying expansion and compression waves generated by flow along a coast can be illustrated through consideration of an irrotational, shallow flow. The governing characteristic equations are developed in Appendix B and we give only a brief recount of the central ideas here. We begin by attempting to cast the steady shallow water equations in a standard quasilinear form (see B1) with two dependent variables. The full shallow water equations, which are normally written in terms of the three variables u , v , and d , may be expressed in terms of just u and v through use of the Bernoulli equation:

$$\frac{u^2 + v^2}{2} + d = d_o. \quad (4.4.1)$$

All variables are now nondimensional, with length, depth, and velocity scales L , D , and $(gD)^{1/2}$. Although the Bernoulli function d_o is normally depends on the streamfunction, it is here rendered constant by the assumption of an irrotational velocity field:

$$\frac{\partial v}{\partial x} - \frac{\partial u}{\partial y} = 0. \quad (4.4.2)$$

If the gradient of (4.4.1) is taken and the continuity equation:

$$d\nabla \cdot \mathbf{u} + \mathbf{u} \cdot \nabla d = 0,$$

is used to eliminate ∇d from the result, one obtains

$$(d - u^2) \frac{\partial u}{\partial x} - uv \left(\frac{\partial u}{\partial y} + \frac{\partial v}{\partial x} \right) + (d - v^2) \frac{\partial v}{\partial y} = 0. \quad (4.4.3)$$

Together, (4.4.2) and (4.4.3) constitute the required form of two equations in the two unknowns u and v , d being considered a function of these variables through (4.4.1).

To achieve the characteristic form, (4.4.2) and (4.4.3) must be linearly combined to form an expression in which all derivatives are expressed in a single direction. This procedure can be carried out successfully provided that the local Froude number $F=(u^2+v^2)^{1/2}/d$ exceeds unity within the region of interest. Under this condition there are two characteristic directions, and the slopes of the corresponding characteristic curves C_+ and C_- are given by

$$\left(\frac{dy}{dx}\right)_{\pm} = \tan(\theta \pm A), \quad (4.4.4)$$

where θ is the inclination of the velocity vector \mathbf{u} with respect to the x -axis and A is the Froude angle defined by

$$d^{1/2} = \pm |\mathbf{u}| \sin A \quad (4.4.5)$$

(see 4.3.2). As sketched in Figure 4.4.1a, the characteristic curves C_+ and C_- at a point P are aligned at angles $\pm A$ with respect to the local velocity vector or streamline. The wedge formed between C_+ and C_- defines the region of downstream influence for P.

Let α and β serve as parameters that vary along the two characteristic curves. Then (4.4.4) implies

$$\cos(\theta + A) \frac{\partial y}{\partial \alpha} = \sin(\theta + A) \frac{\partial x}{\partial \alpha} \text{ along } C_+, \quad (4.4.6a)$$

and

$$\cos(\theta - A) \frac{\partial y}{\partial \beta} = \sin(\theta - A) \frac{\partial x}{\partial \beta} \text{ along } C_-. \quad (4.4.6b)$$

As shown in Appendix B, the characteristic equations governing the evolution of the flow along these curves are given by

$$\sin(\theta - A) \frac{\partial v}{\partial \alpha} = -\cos(\theta - A) \frac{\partial u}{\partial \alpha} \text{ along } C_+, \quad (4.4.7a)$$

and

$$\sin(\theta + A) \frac{\partial v}{\partial \beta} = -\cos(\theta + A) \frac{\partial u}{\partial \beta} \text{ along } C_-. \quad (4.4.7b)$$

If the flow field consists of linearized disturbances to a known background state, then θ and A are known in advance and (4.4.6) can be solved independently to determine the characteristic curves. Equation (4.4.7a,b) can then be integrated along these curves,

beginning from a boundary at which u and v are known, in order to obtain a solution. In more general circumstances, the four equations must be solved simultaneously.

(b) *The hodograph for 2d, irrotational flow.*

A helpful alternative to the physical plane representation of characteristics is the (u,v) plane, or *hodograph*. As suggested in Figure 4.4.1b, the characteristic curves C_+ and C_- have images Γ_+ and Γ_- determined by (4.4.7). Comparing (4.4.6) to (4.4.7), it is apparent that the tangent to C_+ is normal to the tangent Γ_- , and vice versa, when the two directions are represented in the same space. The relationship between A and the angle A' in the (u,v) plane between characteristics and streamlines is thus

$$A' = 90^\circ - A. \quad (4.4.8)$$

It follows from (4.4.5) that

$$d^{1/2} = |(u,v)| \cos(A'). \quad (4.4.9)$$

Hodograph characteristics are inclined at the angle ω with respect to the u -axis, where

$$\omega = \theta + A' \text{ for } \Gamma_+, \quad (4.4.10a)$$

and

$$\omega = \theta - A' \text{ for } \Gamma_-. \quad (4.4.10b)$$

An advantage of the hodograph for two-dimensional, irrotational flow is that the general forms of the characteristic curves can be determined and represented graphically, without regard to the particular geometry or boundary conditions. To determine these forms, it is helpful to introduce the new variables $u^{(n)}$ and $u^{(t)}$ representing the projection of \mathbf{u} normal and tangent to the hodograph characteristic in question. We use the convention that positive $u^{(n)}$ lies to the left of positive $u^{(t)}$. The following analysis applies to either Γ_+ or Γ_- , with ω defined by the corresponding (4.4.10a) or (4.4.10b). The tangential component of the velocity is given by

$$u^{(t)} = u \cos \omega + v \sin \omega = d^{1/2}, \quad (4.4.11)$$

where the final equality follows from (4.4.9). The normal component is given by

$$u^{(n)} = v \cos \omega - u \sin \omega.$$

Rearrangement of these relations leads to

$$u = u^{(t)} \cos \omega - u^{(n)} \sin \omega \quad (4.4.12a)$$

and

$$v = u^{(t)} \sin \omega + u^{(n)} \cos \omega . \quad (4.4.12b)$$

If we now treat ω as a parameter along the Γ_+ or Γ_- curve in question, then differentiation of the last two relations leads to

$$\frac{du}{d\omega} = \frac{du^{(t)}}{d\omega} \cos \omega - \frac{du^{(n)}}{d\omega} \sin \omega - u^{(t)} \sin \omega - u^{(n)} \cos \omega \quad (4.4.13a)$$

and

$$\frac{dv}{d\omega} = \frac{du^{(t)}}{d\omega} \sin \omega + \frac{du^{(n)}}{d\omega} \cos \omega + u^{(t)} \cos \omega - u^{(n)} \sin \omega . \quad (4.4.13b)$$

The combination $\cos(\omega) \times (4.4.13b) - \sin(\omega) \times (4.4.13a)$ leads to

$$\frac{du^{(n)}}{d\omega} = -u^{(t)} , \quad (4.4.14)$$

after use of (4.4.7) with (4.4.10) to eliminate the terms on the left-hand side.

A second equation for $u^{(n)}$ and $u^{(t)}$ can be found from (4.4.11), which allows Bernoulli's relation (4.4.1) to be expressed as

$$\frac{u^{(n)2} + u^{(t)2}}{2} + u^{(t)2} = d_o , \quad (4.4.15)$$

or $\frac{u^{(n)2}}{3} = \frac{2d_o}{3} - u^{(t)2}$. Differentiation of the latter and use of (4.4.14) leads to

$$\frac{du^{(t)}}{d\omega} = \frac{1}{3} u^{(n)} . \quad (4.4.16)$$

The solutions to (4.4.14) and (4.4.16) can be written as

$$u^{(n)} = -(2d_o)^{1/2} \sin \left[(\omega - \omega_o) / \sqrt{3} \right]$$

and

$$u^{(t)} = \left(\frac{2d_o}{3} \right)^{1/2} \cos \left[(\omega - \omega_o) / \sqrt{3} \right] ,$$

where ω_0 is an arbitrary constant. The condition that $u^{(n)}=0$ when $u^{(t)} = (2d_o / 3)^{1/2}$, which follows from (4.4.15), has been imposed. Since Γ_+ may range from lying parallel to the velocity vector ($u^{(n)}=0, u^{(t)}>0$) to lying perpendicular and to the left of the velocity ($u^{(t)}=0, u^{(n)}<0$), $\omega - \omega_0$ can vary over $[0, \sqrt{3}\pi/2]$. Similarly, $\omega - \omega_0$ varies over $[0, -\sqrt{3}\pi/2]$ for Γ_- .

In view of (4.4.12) the solutions for u and v are given by

$$\frac{u}{(2d_o / 3)^{1/2}} = \cos\left[(\omega - \omega_0) / \sqrt{3}\right] \cos \omega + \sqrt{3} \sin\left[(\omega - \omega_0) / \sqrt{3}\right] \sin \omega, \quad (4.4.17a)$$

and

$$\frac{v}{(2d_o / 3)^{1/2}} = \cos\left[(\omega - \omega_0) / \sqrt{3}\right] \sin \omega - \sqrt{3} \sin\left[(\omega - \omega_0) / \sqrt{3}\right] \cos \omega. \quad (4.4.17b)$$

When $\omega = \omega_0$ the above pair give $v / u = \tan \omega_0$, confirming that the hodograph characteristics are aligned with the velocity vector ($A' = 0$). According to (4.5.2) and (4.4.8) this condition requires the Froude number to be unity and ω_0 is therefore the orientation of a particular characteristic under conditions of criticality. If ω is increased from its critical value ω_0 , the hodograph characteristic veers to the left of the velocity vector. The resulting curve should therefore be identified with Γ_+ . Γ_- is generated by decreasing ω below ω_0 .

Since the local Froude number must exceed unity ($u^2 + v^2 > d$) it follows from (4.4.1) that the hodograph characteristics must lie outside the ‘critical’ circle $u^2 + v^2 = 2d_o / 3$, the equivalent of the ‘sonic’ circle in aerodynamics. An outer bound on the range of u and v is the ‘separation circle’ $u^2 + v^2 = 2d_o$ obtained by setting $d = 0$ in (4.4.1). Analogous to the ‘cavitation circle’ in aerodynamics, this bound indicates the flow speed that would occur when the layer depth vanishes, exhausting the available potential energy.

The curves defined by (4.4.17a,b) are epicycloids lying between the critical and separation circles (Figure 4.4.2). These curves can be constructed graphically by considering a point p fixed to the perimeter of the small circle that fits between the bounding circles. If the small circle is rolled around the circumference of the critical (inner) circle, the point p traces out an epicycloid. Figure 4.4.2a shows the curves generated when p initially lies along the critical circle. Rolling the small circle

counterclockwise causes p to move to q ; rolling the circle counterclockwise causes p to move to r . The associated epicycloids Γ_- and Γ_+ are both tangent to (u,v) when the latter touch the critical circle and the direction of the two curves at this point is ω_0 (Figure 4.4.2b). As one moves from p along Γ_+ , the tangent angle ω increases as does the orientation θ of the velocity vector. Since the physical plane characteristic curve C_- is perpendicular to Γ_+ , its angle of inclination $\theta-A$ also increases. The family composed of all possible Γ_- and Γ_+ can be generated by varying the position of the starting point p , or equivalently the angle ω_0 , around the critical circle.

c. Riemann invariants and simple waves.

Now consider the region \mathcal{R} of physical space over which the flow is to be calculated. As an example, we take \mathcal{R} as the area lying downstream of the open boundary \mathcal{B} and to the west of the irregular coastline (Figure 4.4.3a). The flow crossing \mathcal{B} is assumed to be uniform and southward: $d=d_0$ and $u=0$ and $v=v_0$. The C_+ or C_- curves at \mathcal{B} are all inclined at the angle A or $-A$, $A = \sin^{-1}(d_0^{1/2} / v_0)$, relative to the velocity vector. A C_+ curve forms an angle $3\pi/2+A$ with respect to the x -axis while its image Γ_+ forms an angle $(3\pi/2-A)+\pi/2=-A$ in the hodograph. The hodograph image Γ_+ of a particular C_+ curve crossing \mathcal{B} can be found by drawing the velocity vector $\mathbf{u}_0=(0,v_0)$ in the hodograph (Figure 4.4.3b). The desired Γ_+ curve is the one touched by the tip of this vector and is sketched in bold. The uniformity of the flow crossing \mathcal{B} implies that this particular Γ_+ corresponds to *all* the C_+ curves entering \mathcal{R} across \mathcal{B} . A relationship between u and v , say $R_+(u,v)=\text{constant}$, can be constructed by tracing the values along this curve. This relationship must hold over all of \mathcal{R} covered by the C_+ curves originating from the upstream boundary. (In many cases the coverage of \mathcal{R} by these curves is only partial, as when the downstream flow contains shocks.)

The function R_+ is a version of the Riemann invariant discussed in earlier sections in connection with time-dependent flows. Those discussions also alluded to the *simple wave*, a flow region for which one of the Riemann invariants is constant. In the present setting a simple wave corresponds to a region of flow for which all C_+ (or C_-) characteristics correspond to a single Γ_+ (or Γ_-). Since the particular relation between u and v along the unique characteristic holds for the entire simple wave, the individual values of u and v (and therefore d) must be constant along all characteristics of the opposite sign. The slopes of each such characteristic must therefore be constant. In the above example, where all possible u and v values lie along the bold Γ_+ curve (Figure

4.4.3b) the C_- curves must have constant slope. The latter must also lie normal to the bold Γ_+ curve when the two are plotted in the same space.

We now consider the effect of the coastline variation suggested in Figure 4.4.3a. The boundary condition of no normal flow and free slip implies that the inclination θ of the velocity vector at the coast is that of the coast itself. Since the possible range in velocity components u and v is restricted to the bold Γ_+ curve in Figure 4.4.3b, the complete velocity vector \mathbf{u} can be found at each point on the coastline from the local angle θ . If one follows the coastline southward (Figure 4.4.3a) from the upstream boundary (point o) to point m , the value of θ increases from $3\pi/2$ to a slightly larger value. As θ increases, the velocity vector at the coast can be found by tracing along the bold Γ_+ curve in Figure 4.4.3b from o to m . It is clear that the flow speed increases as the point m is reached and that the tilt of the C_- curves, which are perpendicular to Γ_+ , has also increased. The corresponding region of diverging C_- curves, or *expansion fan*, is shown in the upper frame. Further downstream, the coastline bends back southward and the above process is reversed. The result is a set of converging C_- curves that form a shock. The matching conditions appropriate to a shock formed at a simple corner were discussed in the previous section. The Riemann invariant relation between u and v is lost where the C_+ curves cross the dissipative shock. In fact, the dissipation may lead to the generation of vorticity that would invalidate the assumption of a constant Bernoulli function in the downstream region.

The method of characteristics may be used to compute rotating flows, or nonrotating flows with vorticity, but elegant graphical solutions are (apparently) no longer possible. Three characteristic directions and curves must be considered, two of which are defined by (4.4.4) and the third of which are the streamlines. The characteristic equations that must be integrated along these curves to compute the flow are developed in Appendix C and the reader is referred to Garvine (1987) for an application.

Figure Captions

Figure 4.4.1. (a) The wedge of influence for a disturbance generated at the origin in the (x,y) -plane lies between the C_+ and C_- characteristics, which are inclined at the Froude angle A with respect to the velocity vector. In the hodograph (b) the wedge of influence lies between the images of the characteristics Γ_+ and Γ_- , which are inclined at angle A' with respect to the velocity and lie at right angles to C_- and C_+ respectively.

Figure 4.4.2. (a) The critical and separation circles and the epicycloids generated by rolling the small circle on the critical circle. (b) The hodograph characteristics Γ_+ and Γ_- for a particular ω_b .

Figure 4.4.3 (a) Schematic view of the characteristics produced by flow along an irregular coastline. (b): The corresponding hodograph.

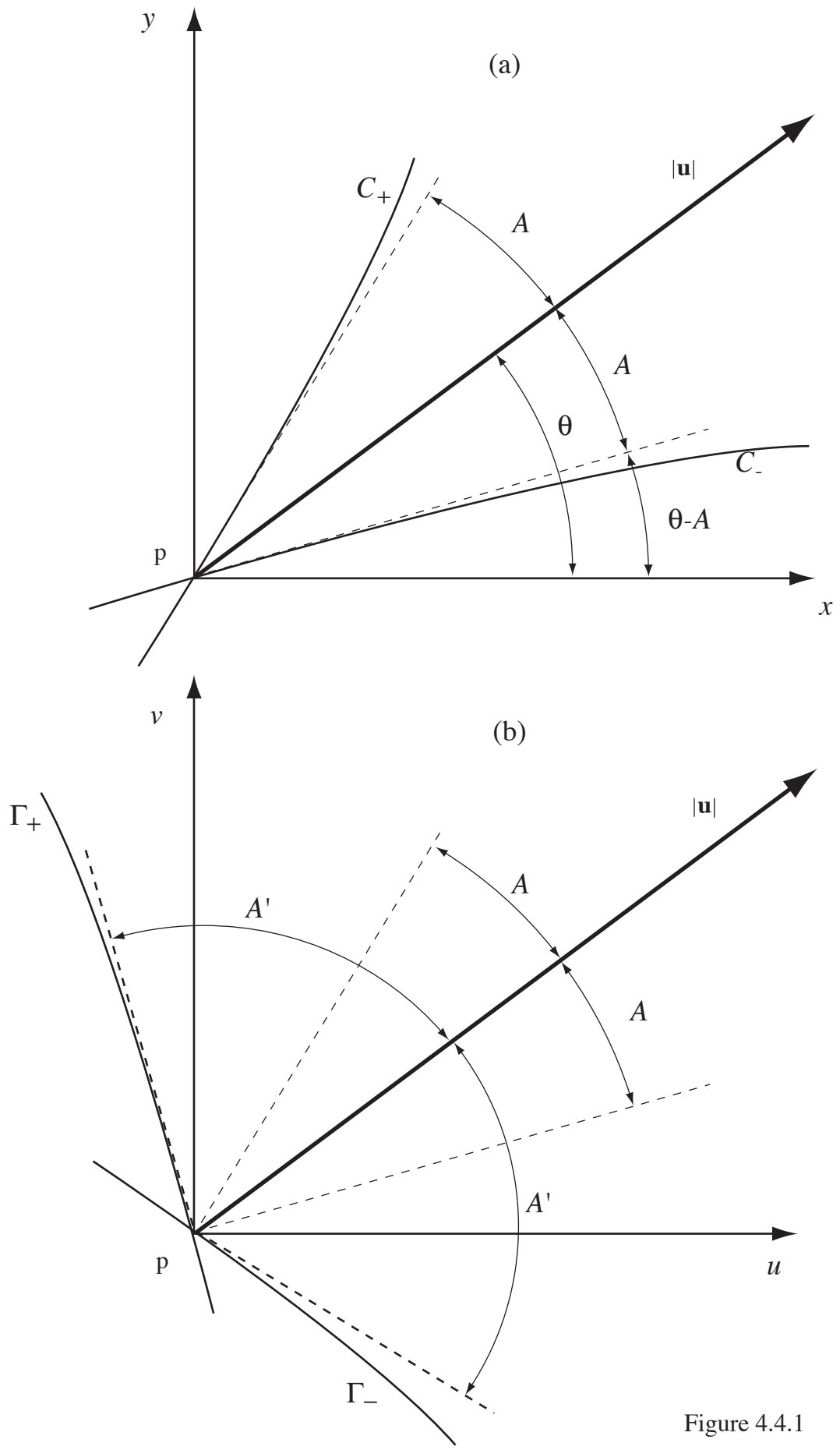


Figure 4.4.1

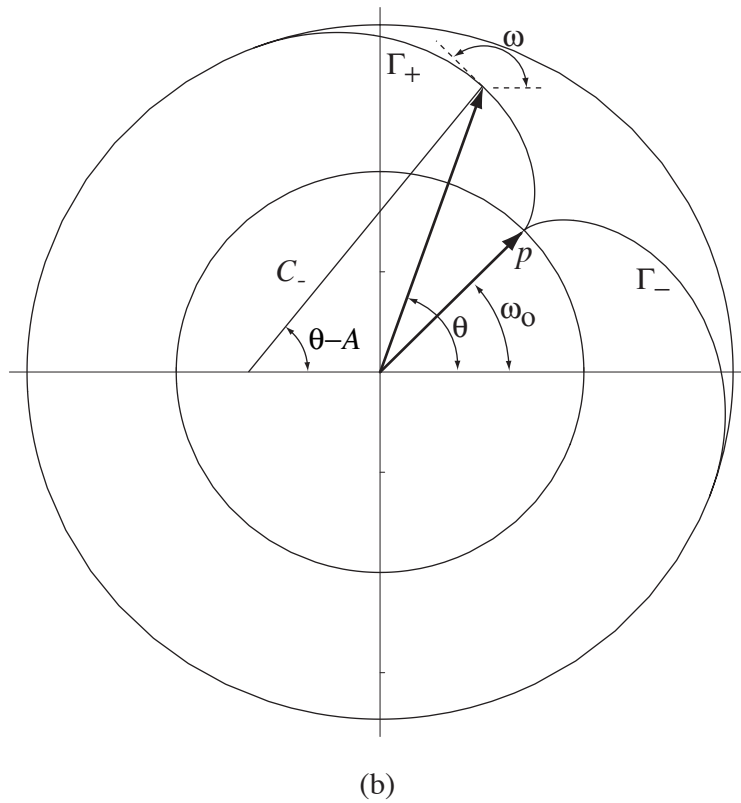
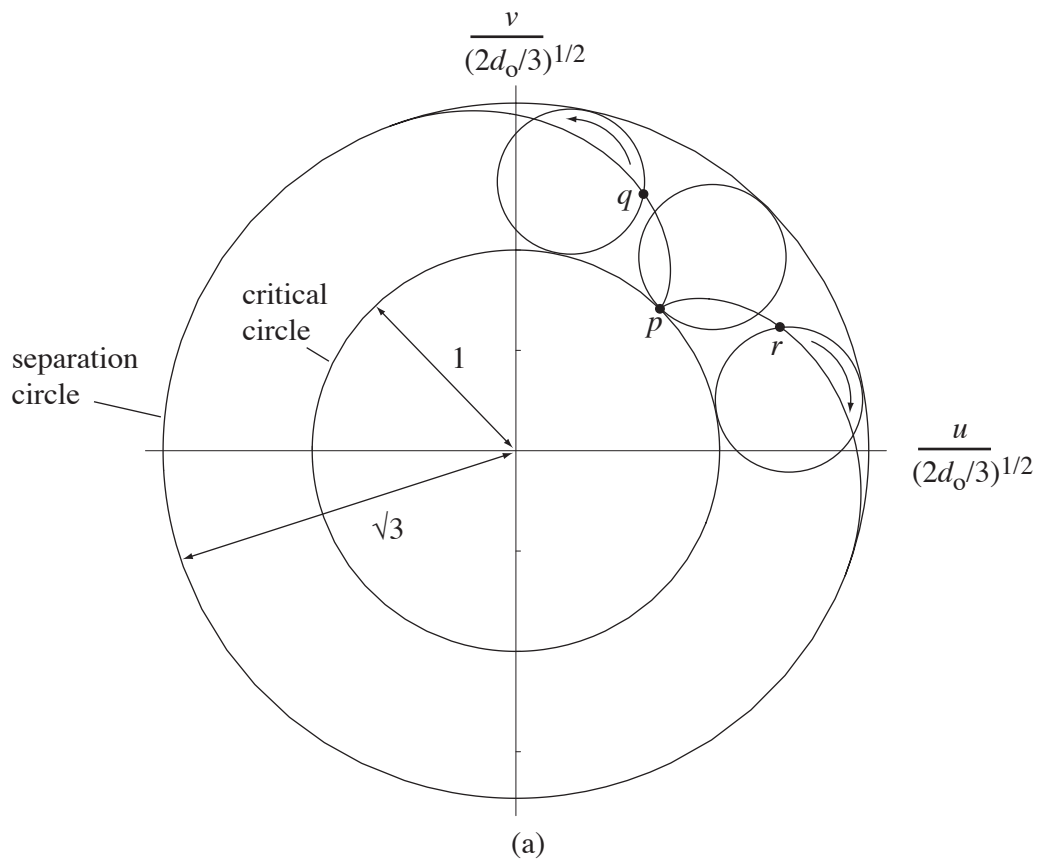
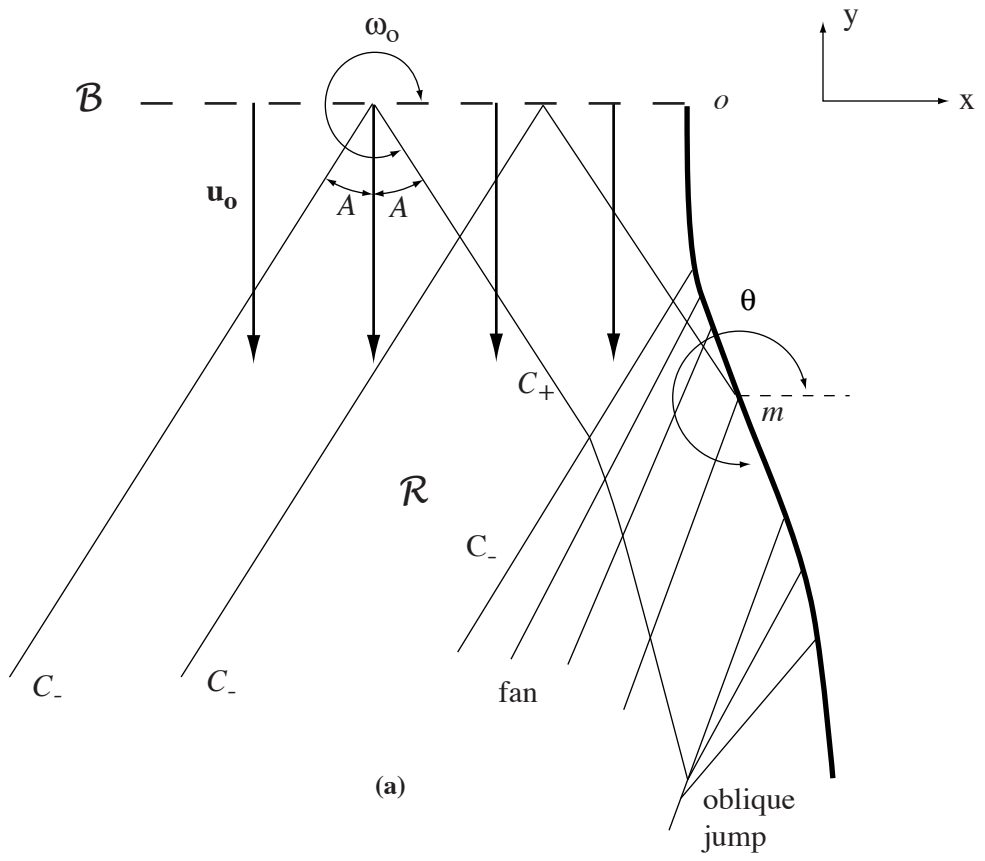
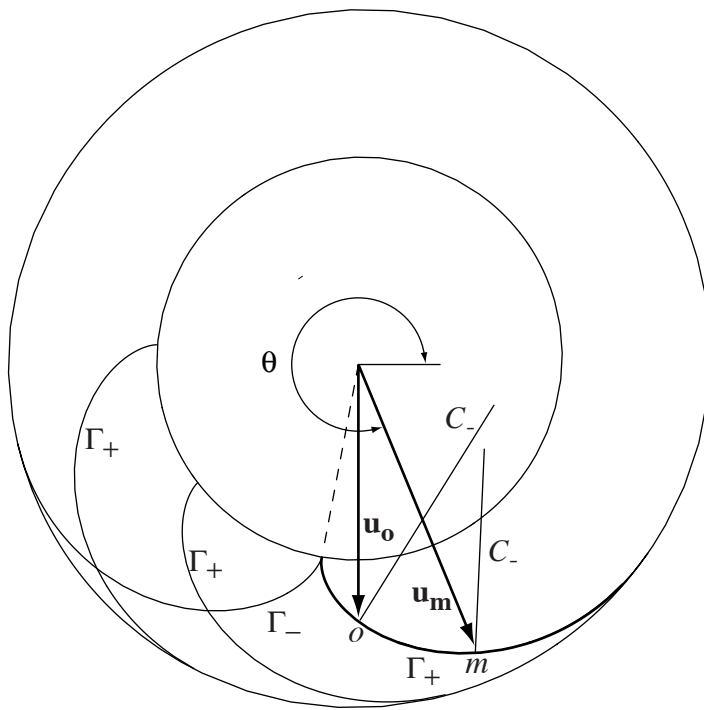


Figure 4.4.2



(a)



(b)

Figure 4.4.3